Transactions of Mathematics and its Applications (2018) **00**, 1–19
doi:10.1093/imatrm/tny001

Holling Type I versus Holling Type II functional responses in Gram-negative bacteria

O. A. Nev and H. A. van den Berg*
University of Warwick, Coventry, CV4 7AL UK
*Corresponding author: hugo@maths.warwick.ac.uk

[Received on 17 July 2017; revised on 8 February 2018]

We consider how the double-membrane structure of the cell envelope of Gram-negative bacteria affects its functional response, which is the mathematical relationship that expresses how the nutrient uptake flux depends on environmental conditions. We show that, under suitable conditions, the Holling Type I functional response is a plausible model, as opposed to the Holling Type II (rectangular hyperbolic, 'Michaelis–Menten') response that is the default model in much of the literature. We investigate both diffusion-limited and capacity-limited regimes. Furthermore, we reconcile our findings with the preponderance in the established literature of hyperbolic models for the growth response, which are generally assumed to be valid, for both Gram-negative and Gram-positive bacteria. Finally, we consider the phenomenon of dynamic adjustment of investment of molecular building blocks in cellular components, and show how this will affect the functional response as observed by the experimenter.

Keywords: Gram-negative bacteria; nutrient uptake; cell envelope; Holling functional response; growth.

1. Introduction

The cell envelope of Gram-negative bacteria consists of two concentric lipid bilayer membranes, an inner membrane (IM) and an outer membrane (OM), in contrast to Gram-positive bacteria that have a single cytoplasmic membrane, corresponding to the IM of the Gram-negative cells (Schlegel & Zaborosch, 1993). While the OM offers an additional layer of protection against a harsh environment, it also poses an additional barrier to substances that the cell requires for growth and metabolism. These molecules must traverse, in turn, first the OM, then the periplasmic space (PS) that lies between IM and OM, and finally enter the cell via the IM. There are three classes of molecular machinery corresponding to these steps: *porins* that mediate transport across the OM, *binding proteins* that capture the molecule while it sojourns in the PS and *transporters* that transport the molecule across the IM (Koebnik *et al.*, 2000; Nikaido, 2003; Davidson & Chen, 2004; Dwyer & Hellinga, 2004). These components are depicted schematically in Fig. 1.

In Gram-positive bacteria, only one membrane needs to be traversed. This allows the flux to be written as a product of two factors, one being a maximum flux that is proportional to the expression level of the transporters, and the other a dimensionless factor that indicates the degree of saturation of the transporter (van den Berg, 2011). The first factor is proportional to the surface density of transporter molecules embedded in the membrane, whereas the second depends on the mechanism of the transporter; a popular choice is the hyperbola that arises in the Michaelis–Menten model (Michaelis & Menten, 1913; Jordy *et al.*, 1996; Button, 1998). In ecology, this hyperbolic response is known as the *Holling Type II* response (Begon *et al.*, 1990). The situation becomes somewhat more involved when

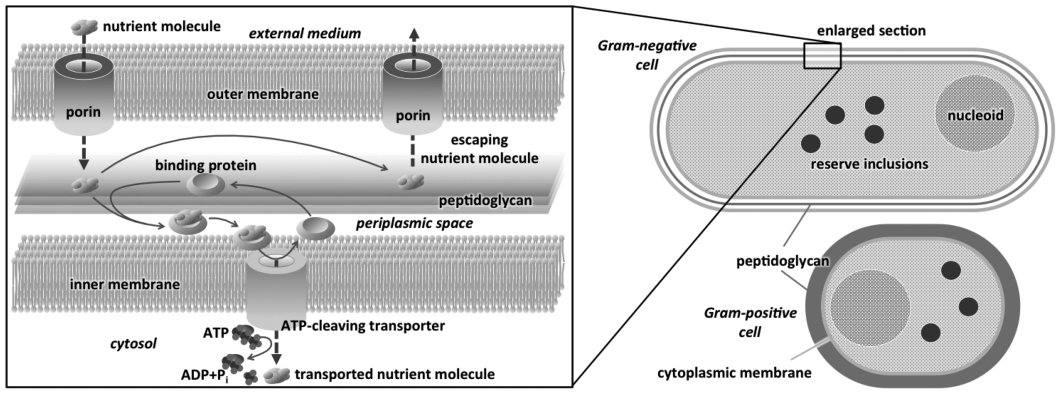

FIG. 1. The dual cell envelope of Gram-negative bacteria (entire cell in cross-section, top right; detail of dual envelope structure, left) compared to the single-membrane envelope of Gram-positive bacteria (bottom-right). In the dual-envelope system, a nutrient molecule may diffuse in through one of the porins that pierces the OM, thus entering the PS, where it can be captured by a binding protein that delivers it to an adenosine triphosphate (ATP)-cleaving transporter, which will translocate the nutrient molecule across the IM (analogous to the cytoplasmic membrane in Gram-positive bacteria). Alternatively, if a nutrient molecule fails to be thus captured, it may eventually escape by diffusing back into the external medium via another porin.

diffusion limitation is taken into account, but even then it is still possible to express the net uptake flux as a function of the density of transporter machinery.

The Gram-negative dual-membrane system, by contrast, is not as readily decomposed into two factors, since the uptake flux depends on the interplay between porins, binding proteins and transporters. Accordingly, the central aim of the present paper is to derive the dependence of the flux on the densities of these three types of machinery. It will be shown that this dependence approximates the *Holling Type I* response (rather than the standard Type II) under certain additional assumptions.

Despite the marked difference in both architecture and functional expressions for the uptake flux, the distinction between single- and dual-membrane uptake systems does not loom large the literature of mathematical models of microbial metabolism and growth. Biomass increase (growth) is essentially a conversion of nutrients into structural biomass; one may conceive of this as a simple (macro-)chemical reaction equation and thus infer that its rate (i.e., the growth rate) should be proportional to the uptake rate. However, we shall demonstrate that this is not necessarily the case, in view of adaptations that the cell can make at the whole-organism level.

2. Dependence of uptake flux on densities of machinery

In Gram-negative bacteria, the pathway that delivers nutrient molecules to the cytosol is composed of (i) porins, which are pore-forming transmembrane proteins that mediate diffusive exchange in both directions between the external medium and the PS, (ii) periplasmic binding proteins that capture the nutrient molecule and deliver it to the final component and (iii) transporters that translocate the nutrient across the IM. The uptake flux per unit membrane surface, Ψ, which has dimensions # nutrient particles $\times$ time^{-1} $\times$ length^2, depends on the densities of all of these three components, and, in addition, on the concentration of the nutrient in the bulk phase of the medium that surrounds the cell. We derive explicit expressions for this flux.

2.1 *Flux conditions for the pores*

Let ρ_{PO} denote the surface density of pores in the OM (with dimensions # porin particles × length^{-2}), r_0 the radius of the cell (dimensions: length), $\widehat{p}$ the permeability of a single pore (which has dimensions: length^3 × time^{-1} × (# porin particles)$^{-1}$) and P_{esc} the probability that a nutrient molecule in the PS that has not yet been captured by a binding protein will find a pore and 'escape' the PS back to the ambient medium, as opposed to encountering a binding protein and binding to it. Let us also write $u(r)$ for the concentration of the nutrient at distance r from the centre of the cell (where u has the dimensions # nutrient particles × length^{-3} and r is a length). Then the uptake flux satisfies the following equation:

$$\Psi = \widehat{p}\rho_{\mathrm{PO}}\left(1 - P_{\mathrm{esc}}\right) u(r_0)\ . \tag{2.1}$$

Assuming diffusive equilibrium outside the cell, we solve the Laplace equation for $u(r)$, as explained in more detail in Section 4.1, and obtain $u(r) = \overline{u} - \alpha/r$, where α is a constant (with dimensions: # nutrient particles × length^{-2}) that remains to be determined and $\overline{u}$ is the bulk ambient concentration of the nutrient. To find α we consider a boundary condition, viz. that the influx must match diffusive supply at $r = r_0$. Thus $\Psi = D\alpha r_0^{-2}$, where D is the nutrient diffusion constant in the ambient medium (dimensions: length^2 × time^{-1}), which can be combined with equation (2.1) to give $\alpha = \overline{u} r_0^2 \left(r_0 + D/(\widehat{p}\rho_{\mathrm{PO}}\left(1 - P_{\mathrm{esc}}\right))\right)^{-1}$. Using this to eliminate α, we find

$$\Psi = \frac{\overline{u}}{r_0/D + \left(\widehat{p}\rho_{\mathrm{PO}}\left(1 - P_{\mathrm{esc}}\right)\right)^{-1}}\ . \tag{2.2}$$

Since $P_{\mathrm{esc}} \in [0, 1]$, we immediately deduce an upper bound on the flux:

$$\Psi \leqslant \frac{\overline{u}}{r_0/D + 1/\left(\widehat{p}\rho_{\mathrm{PO}}\right)}\ . \tag{2.3}$$

If the term r_0/D in the denominator dominates, this upper bound is governed by external diffusive supply, whereas if the term $1/\left(\widehat{p}\rho_{\mathrm{PO}}\right)$ dominates, the flux is limited by porin density. There thus is a critical porin density $\rho_{\mathrm{PO}} \sim D/\left(\widehat{p}r_0\right)$ that marks the transition between the diffusion-limited and capacity-limited regimes.

The escape probability P_{esc} depends on the surface density ρ_{PO} of the porins and the volumetric density $\rho_{\mathrm{BP}}^{\mathrm{free}}$ (dimensions: # binding protein particles × length^{-3}, i.e., concentration) of 'free' binding proteins in the PS, i.e., those whose binding cleft is not occupied by a nutrient molecule. We shall adopt a simple empirical expression for P_{esc}:

$$P_{\mathrm{esc}} = \left(1 + \delta\rho_{\mathrm{BP}}^{\mathrm{free}}/\rho_{\mathrm{PO}}\right)^{-1}\ , \tag{2.4}$$

where δ is a parameter with the dimensions of a length; Section 4.2 provides a detailed heuristic argument for this formula. Using equation (2.4) to eliminate P_{esc} from equation (2.2), we obtain a relationship between flux and the densities of porins and free binding proteins:

$$\rho_{\mathrm{BP}}^{\mathrm{free}} = \frac{\delta^{-1}}{\widehat{p}\left(\overline{u}/\Psi - r_0/D\right) - 1/\rho_{\mathrm{PO}}}\ . \tag{2.5}$$

The binding proteins satisfy a conservation principle:

$$\rho_{\mathrm{BP}} = \rho_{\mathrm{BP}}^{\mathrm{free}} + \rho_{\mathrm{BP}}^{\mathrm{bound}}\,, \tag{2.6}$$

where $\rho_{\mathrm{BP}}^{\mathrm{bound}}$ is the volumetric density of nutrient-charged binding proteins in the PS and ρ_{BP} is the total density. Equations (2.5) and (2.6) allow us to describe how the flux Ψ depends on the ambient bulk concentration $\bar{u}$, given the machinery densities ρ_{PO}, ρ_{BP} and ρ_{TR} (the latter having dimensions # transporter particles × length^{-2}); all that remains to be determined is a condition that fixes $\rho_{\mathrm{BP}}^{\mathrm{bound}}$.

The porins are here treated as passive devices; thus the net exchange flux they mediate is analogous to the net flux across a semi-permeable membrane, with permeability $\widehat{p}\rho_{\mathrm{PO}}$, suspended between two well-mixed bulk phases with concentrations u_{A} and u_{B}; in particular, the net flux per unit membrane surface, in the direction of the 'A' side, is then given by the formula $\widehat{p}\rho_{\mathrm{PO}}\left(u_{\mathrm{A}} - u_{\mathrm{B}}\right)$. Thus, we are supposing that $P_{\mathrm{esc}}u(r_0)$ represents the effective concentration of free nutrient molecules in the PS. The presumed passive nature of the porins is the reason that our approach differs from (but is not inconsistent with) that followed in the seminal paper by Berg & Purcell (1977) whose 'ideally absorptive patches' treatment calls for a consideration of surface diffusion effects; this approach is well-suited for both receptors and active transporters. In the present scenario, the active transporters are situated on the periplasmic surface of the IM (Fig. 1). As will become clear in the next section, we shall be concerned with capture by binding proteins as the bottle-neck step, and our treatment of this problem has commonalities with that of Berg & Purcell (1977).

2.2 *Flux conditions for the transporters*

Let ρ_{TR} denote the surface density of transporters in the IM and $\widehat{\psi}$ the maximum flux that can be carried by a single transporter. This gives a second upper bound on the flux: $\Psi \leqslant \rho_{\mathrm{TR}}\widehat{\psi}$. The expected proportion of transporters that is actively translocating a nutrient at a given moment in time equals the dimensionless engagement fraction $\Psi/(\rho_{\mathrm{TR}}\widehat{\psi})$. This fraction can alternatively be deduced from the transporter's cycle time statistics, and combining these gives another condition on the flux and machinery densities.

In particular, consider that it takes a transporter, on average, an amount of time T_{lig} to first ligate a binding protein, then process the nutrient molecule (if the binding protein is charged), and, finally, release the binding protein. If the binding proteins perform statistically independent random walks through the PS and are present at a constant concentration in the PS, the arrival of binding proteins at a certain transporter can be modelled as a Poisson process, the time between events in such a process is described by the exponential distribution with a parameter λ (with dimension time^{-1}), and thus the mean waiting time equals $1/\lambda$. The rate λ is the sum of the encounter rates for free and bound binding proteins in the PS, each term being proportional to the density of the corresponding species. Thus $\lambda = \lambda^{\mathrm{free}}\rho_{\mathrm{BP}}^{\mathrm{free}} + \lambda^{\mathrm{bound}}\rho_{\mathrm{BP}}^{\mathrm{bound}}$, where λ^{free} and λ^{bound} are rate parameters with dimensions length^3 × time^{-1} × (# binding protein particles)$^{-1}$. The expected duration of a cycle is found by adding the average times for the two phases:

$$T_{\mathrm{cyc}} = T_{\mathrm{lig}} + \left(\lambda^{\mathrm{free}}\rho_{\mathrm{BP}}^{\mathrm{free}} + \lambda^{\mathrm{bound}}\rho_{\mathrm{BP}}^{\mathrm{bound}}\right)^{-1}\,. \tag{2.7}$$

The fraction of transporters that will be actively engaged at any given moment in time can be expressed as $\mathbb{P}\,T_{\mathrm{lig}}/T_{\mathrm{cyc}}$, where $\mathbb{P}$ is a probability that a transporter binds a binding protein with cargo. This

probability can be expressed as follows:

$$\mathbb{P} = \frac{\lambda^{\text{bound}}\rho_{\text{BP}}^{\text{bound}}}{\lambda^{\text{free}}\rho_{\text{BP}}^{\text{free}} + \lambda^{\text{bound}}\rho_{\text{BP}}^{\text{bound}}} = \left(1 + \beta\rho_{\text{BP}}^{\text{free}}/\rho_{\text{BP}}^{\text{bound}}\right)^{-1} , \tag{2.8}$$

where $\beta = \lambda^{\text{free}}/\lambda^{\text{bound}}$. If we define two auxiliary quantities as follows:

$$\rho_{\text{C}}^{\text{free}} = \left(\lambda^{\text{free}}T_{\text{lig}}\right)^{-1} \quad \text{and} \quad \rho_{\text{C}}^{\text{bound}} = \left(\lambda^{\text{bound}}T_{\text{lig}}\right)^{-1} , \tag{2.9}$$

we find that the dimensionless quantity $T_{\text{lig}}/T_{\text{cyc}}$ can be written as

$$\left(\rho_{\text{BP}}^{\text{free}}/\rho_{\text{C}}^{\text{free}} + \rho_{\text{BP}}^{\text{bound}}/\rho_{\text{C}}^{\text{bound}}\right) / \left(1 + \rho_{\text{BP}}^{\text{free}}/\rho_{\text{C}}^{\text{free}} + \rho_{\text{BP}}^{\text{bound}}/\rho_{\text{C}}^{\text{bound}}\right) .$$

We now have two expressions for the fraction of engaged transporters, namely $\Psi/(\rho_{\text{TR}}\widehat{\psi})$ and $\mathbb{P}\,T_{\text{lig}}/T_{\text{cyc}}$. Equating these we have

$$\frac{\Psi}{\rho_{\text{TR}}\widehat{\psi}} = \frac{\rho_{\text{BP}}^{\text{free}}/\rho_{\text{C}}^{\text{free}} + \rho_{\text{BP}}^{\text{bound}}/\rho_{\text{C}}^{\text{bound}}}{1 + \rho_{\text{BP}}^{\text{free}}/\rho_{\text{C}}^{\text{free}} + \rho_{\text{BP}}^{\text{bound}}/\rho_{\text{C}}^{\text{bound}}} \left(1 + \beta\rho_{\text{BP}}^{\text{free}}/\rho_{\text{BP}}^{\text{bound}}\right)^{-1} . \tag{2.10}$$

The compound parameters $\rho_{\text{C}}^{\text{free}}$ and $\rho_{\text{C}}^{\text{bound}}$ have the same dimensions as $\rho_{\text{BP}}^{\text{free}}$ (i.e., volumetric density, # binding protein particles × length^{-3}) and can be interpreted as saturation parameters for the transporter in terms of its cargo, somewhat akin to the familiar parameter K_m in the Michaelis–Menten equation.

2.3 *Flux when the transporter only binds nutrient-loaded binding proteins*

The first special case we shall consider arises when the transporters do not ligate free binding proteins, i.e., $\lambda^{\text{free}} = 0$ and $\beta = 0$. In this case solving equation (2.10) for $\rho_{\text{BP}}^{\text{bound}}$ gives a simple formula:

$$\rho_{\text{BP}}^{\text{bound}} = \rho_{\text{C}}^{\text{bound}} \frac{\Psi}{\rho_{\text{TR}}\widehat{\psi} - \Psi} . \tag{2.11}$$

With equations (2.5) and (2.6), we obtain

$$\rho_{\text{BP}} = \frac{(\delta\widehat{p})^{-1}}{\overline{u}/\Psi - \left(r_0/D + 1/(\widehat{p}\rho_{\text{PO}})\right)} + \frac{\rho_{\text{C}}\Psi}{\rho_{\text{TR}}\widehat{\psi} - \Psi} , \tag{2.12}$$

where we have written ρ_{C} for $\rho_{\text{C}}^{\text{bound}}$. The obvious next step is to solve equation (2.12) for Ψ, since it is Ψ that depends on $\overline{u}$ (given the machinery densities), but a better insight into the nature of the solution can be gleaned if we make $\overline{u}$ the subject of the equation:

$$\overline{u} = \Psi\left(\frac{r_0}{D} + \frac{1}{\widehat{p}\rho_{\text{PO}}}\right) + \frac{\Psi}{\rho_{\text{C}}\widehat{p}\delta\left(\rho_{\text{BP}}/\rho_{\text{C}} + \left(\rho_{\text{TR}}\widehat{\psi}/\Psi - 1\right)^{-1}\right)} . \tag{2.13}$$

The second term on the right diverges at $\Psi = \rho_{\mathrm{TR}}\widehat{\psi}/(1-\rho_{\mathrm{C}}/\rho_{\mathrm{BP}})$, which means that

$$\lim_{\overline{u}\to\infty}\Psi = \frac{\rho_{\mathrm{TR}}\widehat{\psi}}{1-\rho_{\mathrm{C}}/\rho_{\mathrm{BP}}} \approx \rho_{\mathrm{TR}}\widehat{\psi}\,, \tag{2.14}$$

with the latter term obtaining in the case $\rho_{\mathrm{BP}} \gg \rho_{\mathrm{C}}$; thus, if the binding proteins are present in excess (relative to the critical density ρ_{C}), the transporter-dependent maximum $\rho_{\mathrm{TR}}\widehat{\psi}$ governs the uptake flux at sufficiently large values of the bulk concentration $\overline{u}$.

Moreover, in the case of binding protein excess ($\rho_{\mathrm{BP}} \gg \rho_{\mathrm{C}}$), the second term in equation (2.13) is dominated by the first term when Ψ is well below its transporter-dependent maximum, so that $\Psi \ll \rho_{\mathrm{TR}}\widehat{\psi}$. Thus we deduce that Ψ as a function of $\overline{u}$ consists of a linear portion

$$\Psi \approx \left(\frac{r_0}{D} + \frac{1}{\widehat{p}\rho_{\mathrm{PO}}}\right)^{-1}\overline{u}\,, \tag{2.15}$$

followed by a constant portion $\Psi \approx \rho_{\mathrm{TR}}\widehat{\psi}$, with a transition at $\overline{u} \approx \left(r_0/D + (\widehat{p}\rho_{\mathrm{PO}})^{-1}\right)\rho_{\mathrm{TR}}\widehat{\psi}$. These approximations become better as ρ_{BP} increases, and in the limit $\rho_{\mathrm{BP}} \to \infty$ the Ψ-$\overline{u}$ graph consists of these two straight line segments, that is, we have obtained the classic *Holling Type I functional response*. An absolute upper bound is furnished by the diffusion-limited flux $\Psi = D\overline{u}/r_0$; this flux coincides with the initial portion in an additional limiting case, viz. when the porins are also present in excess.

The idealised Type I response has a property that is illustrated in Fig. 2: at a given bulk concentration $\overline{u}$, the uptake flux will equal $\rho_{\mathrm{TR}}\widehat{\psi}$ as long as $\rho_{\mathrm{TR}} \leqslant \overline{\rho_{\mathrm{TR}}}$, where

$$\overline{\rho_{\mathrm{TR}}} = \overline{u}\left(r_0/D + (\widehat{p}\rho_{\mathrm{PO}})^{-1}\right)^{-1}\widehat{\psi}^{-1}\,. \tag{2.16}$$

For $\rho_{\mathrm{TR}} > \overline{\rho_{\mathrm{TR}}}$ the flux will lie on the initial portion of the response and be dependent on the porin density only. Thus, as the cell increases its transporter density, it will abruptly switch from maximally engaged transporters (below the critical density $\overline{\rho_{\mathrm{TR}}}$) to a situation where adding transporters does not further enhance the flux.

2.4 *Flux when the transporter binds free and bound binding proteins with equal affinity*

A second special case arises when the transporters ligate free binding proteins with the same kinetics as nutrient-loaded binding proteins, i.e., $\lambda^{\mathrm{free}} = \lambda^{\mathrm{bound}}$, $\beta = 1$ and $\rho_{\mathrm{C}}^{\mathrm{free}} = \rho_{\mathrm{C}}^{\mathrm{bound}} = \rho_{\mathrm{C}}$. The counterpart to equation (2.13) in this case is as follows:

$$\overline{u} = \Psi\left(\frac{r_0}{D} + \frac{1}{\widehat{p}\rho_{\mathrm{PO}}}\right) + \frac{\Psi}{\rho_{\mathrm{C}}\widehat{p}\delta\left(\rho_{\mathrm{BP}}/\rho_{\mathrm{C}} - \left(1+\rho_{\mathrm{BP}}/\rho_{\mathrm{C}}\right)\Psi/(\rho_{\mathrm{TR}}\widehat{\psi})\right)}\,, \tag{2.17}$$

which virtually agrees with equation (2.13) in the case $\rho_{\mathrm{BP}} \ll \rho_{\mathrm{C}}$. Furthermore, the flux supremum, equation (2.14), applies here as well, and again the Ψ-$\overline{u}$ graph approaches the Holling Type I functional response as a limiting case as $\rho_{\mathrm{BP}} \to \infty$, although the convergence is substantially slower.

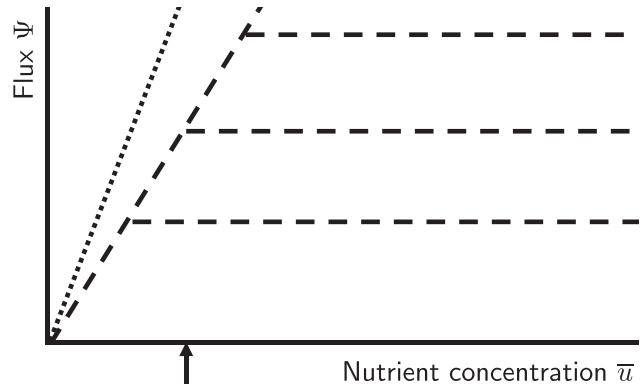

FIG. 2. The Type I response characteristic of the dual-envelope microbial nutrient uptake system. The flux Ψ as a function of bulk nutrient concentration $\bar{u}$ has a graph consisting of a slanted straight line segment followed by a horizontal line segment; the level of the latter increases in direct proportion to the transporter density ρ_{TR}; three different levels are shown by dashed lines, with the transition in each case occurring where the dashed slanted line intersects. Thus, at the nutrient concentration indicated by the arrow, flux Ψ will increase in proportion to ρ_{TR} until the level indicated by the middle line is reached, and any increases in ρ_{TR} beyond that point do not affect Ψ. The slope of the slanted line is governed by the porin density ρ_{PO}; as the latter increases, the slanted segment converges to the dotted line, which is an absolute upper bound determined by diffusion limitation.

3. Functional responses at the whole-organism level: the growth response

In as much as nutrients are converted into biomass, it is tempting to take growth, defined as the rate of increase of biomass, to be proportional to this flux; the functional response then does double duty as the assimilatory response and as a linker function in the population dynamics. Such is indeed the case in elementary mathematical models of ecological theory (Begon *et al.*, 1990; van den Berg, 2011). In the study of bacterial growth, the dependence of the specific growth rate ($\mu = \frac{d}{dt} \ln W(t)$ where $W(t)$ denotes biomass; regardless of the dimensions chosen for W, μ is a pure rate, i.e., time^{-1}) on bulk nutrient concentration u is usually described by a hyperbola. Thus, the canonical growth response model is represented by the equation

$$\mu = \widehat{\mu}/(1 + K_{\mu}/u) \,, \tag{3.1}$$

where $\widehat{\mu}$ and K_{μ} are positive parameters and u denotes the bulk concentration of the (limiting) nutrient (K_{μ} has the same dimensions as u); this model is often employed alongside the standard functional response model, $\Psi = \widehat{\Psi}/(1 + K_{\Psi}/u)$, with positive parameters $\widehat{\Psi}$ and K_{Ψ}. In view of their analogous mathematical roles, one might equate K_{μ} to K_{Ψ}, but in fact $K_{\mu} \ll K_{\Psi}$ is often the case, as was already pointed out by Monod (1949) who pioneered this approach. The model has since extended to accommodate the phenomena of maintenance requirements (Pirt, 1965; Marr *et al.*, 1962) and variable internal stores (Droop, 1968; Grover, 1991; Kooijman, 2009), but its essential hyperbolic character has endured.

In this section, we will argue that hyperbolic 'whole-organism' (i.e., growth) responses are to be expected, even when the functional response of nutrient uptake is Holling Type I. The essence of our argument resides in the fact that microorganisms regulate and adjust the investment of cellular resources, that is, the allocation of molecular building blocks towards the various types of catalytic machinery that a cell is capable to express. The importance of this investment profile and its dynamic nature has been recognised for some time now (Kramer *et al.*, 2010; Li *et al.*, 2014; Liebermeister *et al.*, 2014). We shall

show that optimal allocation strategies tend to engender hyperbolic responses at the whole-organism level.

To keep the analysis as straightforward as possible, we shall confine ourselves to balanced assimilation, that is, nutrient uptake that matches the requirements in stoichiometric terms. In particular, since biomass has a fixed compositional stoichiometry, it follows that the uptake fluxes of a given pair of nutrients, say Ψ_A and Ψ_B, should be such that their ratio Ψ_A/Ψ_B is a fixed constant that agrees with the stoichiometric requirements of biomass production. If Ψ_A/Ψ_B deviates from this constant, there will be a surplus of either nutrient A or nutrient B that the cell can dispose of by generating reserves (incorporating the surplus into cellular inclusions), or by secreting the surplus into the ambient medium, or by modifying the transporter that carries the nutrient in surplus, so that it operates at a reduced degree of efficiency. What these three strategies have in common is that they all reduce the rate of growth that can be achieved, compared to the rate of growth that would have been possible if the uptake fluxes Ψ_A and Ψ_B had been adapted to stoichiometric requirements outright. This provides a biological rationale for supposing, at least on the face of it, that microorganisms effect such adaptation, and leads us to investigate how they might achieve such balancing.

3.1 *Balancing when machinery is limiting*

Let us first consider the case where diffusion limitation is not a factor, i.e., the r_0/D term in equations (2.13) and (2.17) is negligibly small compared to the $1/(\widehat{p}\rho_{PO})$ term. We also assume that binding proteins are always present in excess, so that we have the Type I response as depicted in Fig. 2 for both nutrients.

Under these assumptions, maximum growth is achieved when both uptake systems are residing at the transition point between the increasing and constant sections of the Type I response. To see this, fix the environment (i.e., fix two values $\overline{u}_A$ and $\overline{u}_B$) and consider the fluxes Ψ_A and Ψ_B as a function of the transporter densities $\rho_{TR\cdot A}$ and $\rho_{TR\cdot B}$. The relevant geometry of the $(\rho_{TR\cdot A}, \rho_{TR\cdot B})$-plane is represented in Fig. 3(a). The region where the flux is porin-limited is indicated in grey (the transition from transporter to porin-limitation is explained in Fig. 2; see Section 2.3), so that in this region we have $\rho_{TR\cdot A} > \overline{\rho_{TR\cdot A}}$ and $\rho_{TR\cdot B} > \overline{\rho_{TR\cdot B}}$, where $\overline{\rho_{TR\cdot A}}$ and $\overline{\rho_{TR\cdot B}}$ are defined by equation (2.16) in the absence of diffusion

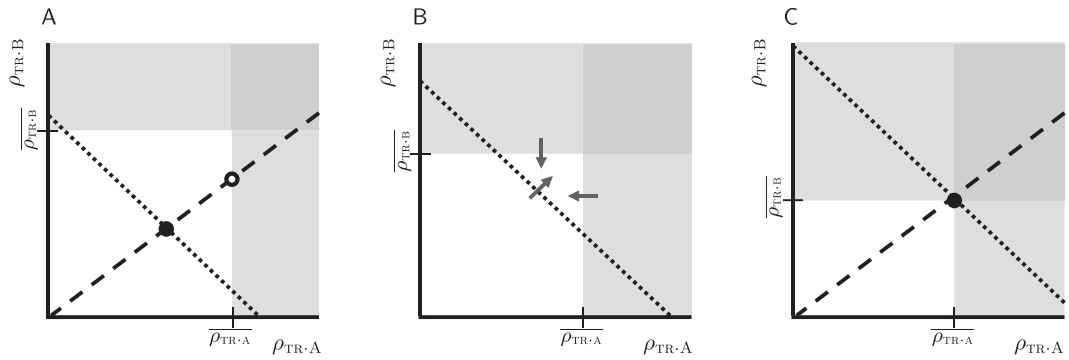

FIG. 3. Schematic illustrating the effects of trading off building blocks investment into porins and transporters. Further explanation in the text.

limitation factor as follows:

$$\overline{\rho_{\mathrm{TR\cdot A}}} = \overline{u}_{\mathrm{A}}\widehat{p_{\mathrm{A}}}\rho_{\mathrm{PO\cdot A}}\widehat{\psi_{\mathrm{A}}}^{-1}\,, \qquad \overline{\rho_{\mathrm{TR\cdot B}}} = \overline{u}_{\mathrm{B}}\widehat{p_{\mathrm{B}}}\rho_{\mathrm{PO\cdot B}}\widehat{\psi_{\mathrm{B}}}^{-1}\,. \tag{3.2}$$

The increasing dashed line indicates the balanced condition; if $(\rho_{\mathrm{TR\cdot A}},\rho_{\mathrm{TR\cdot B}})$ is chosen below this line, nutrient A will accumulate (or must be sluiced off), and *vice versa* for $(\rho_{\mathrm{TR\cdot A}},\rho_{\mathrm{TR\cdot B}})$ above this line (this is correct only for the transporter-limited regime, that is, along the increasing dashed line between the origin and the point marked with an open circle). If a total 'budget' of molecular building blocks is to be divided among transporters for A and B, the system will be positioned somewhere along the decreasing dotted line, which can be regarded as representing the trade-off of investment of molecular building blocks. The intersection of the dashed and dotted lines (black dot) thus indicates the balanced growth allocation of building blocks towards the two types of transporters.

However, the cell allocates building blocks among the porins and the transporters. In this case the budget for transporters can be augmented by taking a portion away from the porin budget. The effect of such an exchange is supported by equation (3.2) and is illustrated in Fig. 3(b). The boundaries of the grey regions shift towards the origin as the porin density decreases. Performing a series of such allocation shifts from the porin budget to the transporter budget, the system can keep 'climbing' in this manner, moving upwards along the dashed line on which nutrient uptake and growth requirements are balanced. The logical end point is depicted in Fig. 3(c): the 'climb' terminates when the boundaries of the grey regions just touch the dotted allocation line.

Let us momentarily suppose that the specific growth rate μ depends only on the availabilities of nutrients A and B. In the case represented by Fig. 3(c), we find that μ is proportional to both Ψ_{A} and Ψ_{B}. Therefore μ is also simultaneously proportional to $\rho_{\mathrm{TR\cdot A}}$, $\rho_{\mathrm{TR\cdot B}}$, $\rho_{\mathrm{PO\cdot A}}\overline{u}_{\mathrm{A}}$ and $\rho_{\mathrm{PO\cdot B}}\overline{u}_{\mathrm{B}}$:

$$\mu = k_{\mathrm{TR\cdot A}}\rho_{\mathrm{TR\cdot A}} = k_{\mathrm{TR\cdot B}}\rho_{\mathrm{TR\cdot B}} = k_{\mathrm{PO\cdot A}}\rho_{\mathrm{PO\cdot A}}\overline{u}_{\mathrm{A}} = k_{\mathrm{PO\cdot B}}\rho_{\mathrm{PO\cdot B}}\overline{u}_{\mathrm{B}}\,, \tag{3.3}$$

where the coefficients $k_{\mathrm{TR\cdot A}}$,$k_{\mathrm{TR\cdot B}}$,$k_{\mathrm{PO\cdot A}}$,$k_{\mathrm{PO\cdot B}}$ are positive stoichiometric parameters. The coefficients $k_{\mathrm{PO\cdot A}}$ and $k_{\mathrm{PO\cdot B}}$ have dimensions length^5 × (# porin particles)$^{-1}$ × (# nutrient particles)$^{-1}$ × time^{-1}. The coefficients $k_{\mathrm{TR\cdot A}}$ and $k_{\mathrm{TR\cdot B}}$ have dimensions length^2 × (# transporter particles)$^{-1}$ × time^{-1}.

Furthermore, budgeting of building blocks for these four types of machinery imposes a linear constraint of the following form:

$$c_{\mathrm{TR\cdot A}}\rho_{\mathrm{TR\cdot A}} + c_{\mathrm{TR\cdot B}}\rho_{\mathrm{TR\cdot B}} + c_{\mathrm{PO\cdot A}}\rho_{\mathrm{PO\cdot A}} + c_{\mathrm{PO\cdot B}}\rho_{\mathrm{PO\cdot B}} = C\,, \tag{3.4}$$

where $c_{\mathrm{TR\cdot A}}$, $c_{\mathrm{TR\cdot B}}$, $c_{\mathrm{PO\cdot A}}$, $c_{\mathrm{PO\cdot B}}$ are positive stoichiometric parameters and C is a positive constant. The coefficients $c_{\mathrm{PO\cdot A}}$ and $c_{\mathrm{PO\cdot B}}$ have dimensions length^2 × (# porin particles)$^{-1}$. The coefficients $c_{\mathrm{TR\cdot A}}$ and $c_{\mathrm{TR\cdot B}}$ have dimensions length^2 × (# transporter particles)$^{-1}$.

Combining the proportionality relations defined by equation (3.3) with equation (3.4), we infer that the growth rate satisfies

$$\frac{1}{\mu} = \frac{1}{\widehat{\mu}} + \frac{\gamma_{\mathrm{A}}}{\overline{u}_{\mathrm{A}}} + \frac{\gamma_{\mathrm{B}}}{\overline{u}_{\mathrm{B}}}\,, \tag{3.5}$$

where $\widehat{\mu}$, γ_{A} and γ_{B} are positive compound parameters that absorb various stoichiometric coefficients and 'cost' factors from equations (3.3) and (3.4). The coefficients γ_{A} and γ_{B} have dimensions # nutrient particles × length^{-3} × time.

However, we should only expect equation (3.5) to hold good under steady state conditions, when the cell has had the opportunity to re-allocate building blocks to the various types of machinery. Equation (3.5) states that μ depends on either nutrient in the hyperbolic fashion; we may rewrite this equation as a dependence on $\overline{u}_{\mathrm{A}}$ (say) in the two-parameter form of equation (3.1), but the *apparent* parameters $\widehat{\mu}$ and K_{μ} in equation (3.1) are then seen to be functions of $\overline{u}_{\mathrm{B}}$, of course. In particular, if care was taken to ensure that this nutrient was not limiting (i.e., $\overline{u}_{\mathrm{B}} \gg \widehat{\mu}\gamma_{\mathrm{A}}$) then $K_{\psi,\mathrm{B}} = \widehat{\mu}\gamma_{\mathrm{B}}$. The argument given here can be readily generalised to three or more essential nutrients, yielding the following expression for μ:

$$\frac{1}{\mu} = \frac{1}{\widehat{\mu}} + \sum_{i=1}^{n} \frac{\gamma_i}{\overline{u}_i} \,, \tag{3.6}$$

where n is the number of essential nutrients.

3.2 *Balancing when diffusion is limiting*

We next consider the opposite extreme case where the diffusion term dominates. In this case the transition marked by the boundary of the grey region in Fig. 3 depends on $D_{\mathrm{A}}\overline{u}_{\mathrm{A}}$ and $D_{\mathrm{B}}\overline{u}_{\mathrm{B}}$ and is virtually independent of re-allocation of molecular building blocks towards the porins. The maximum balanced flux point is therefore the one marked by the open circle in Fig. 3(a) and the steady-state dependence of the specific growth rate on the nutrient concentrations takes on the following form:

$$\mu = \min\left\{\varkappa_{\mathrm{A}}\overline{u}_{\mathrm{A}}, \varkappa_{\mathrm{B}}\overline{u}_{\mathrm{B}}\right\} \,, \tag{3.7}$$

where $\varkappa_{\mathrm{A}}$ and $\varkappa_{\mathrm{B}}$ are positive compound parameters that absorb various stoichiometric coefficients and 'cost' factors, and have dimensions (# nutrient particles)$^{-1}$ × length^3 × time^{-1}.

The minimum model represented by equation (3.7), which is well established in the microbiological literature (Gottschal, 1992), generalises in the obvious manner to n essential nutrients:

$$\mu = \min\left\{\varkappa_1\overline{u}_1, \ldots, \varkappa_n\overline{u}_n\right\} \,. \tag{3.8}$$

The present analysis suggests that the minimum model and the hyperbolic model, equation (3.6), are both physiologically plausible and compatible with the same underlying machinery. That is to say, they are not rival models but could both be valid for a given bacterial species, depending on whether or not the data were obtained under diffusion-limited conditions.

This observation implies that results obtained under laboratory conditions should be applied to the field with due caution. For instance, diffusion limitation may well prevail in the organism's ecological habitat, whereas its characteristic properties have been determined in a chemostat apparatus, in which diffusion limitation may be less important. An analysis along the present lines will allow micro-ecologists to translate parameter estimates obtained in the laboratory into the parameter values required for the 'field-equivalent' model.

3.3 *Comparison to single-layer envelope cells*

In the single-envelope system, such as found in Gram-positive bacteria, the transporters communicate directly with the ambient medium. Let us assume that the transport system obeys the Michaelis–Menten

equation:

$$\Psi = \rho_{\mathrm{TR}} \widehat{\psi} \frac{u(r_0)}{K_m + u(r_0)} , \tag{3.9}$$

where K_m is the 'half-saturation' parameter and $u(r_0) = \overline{u} - \alpha / r_0$ for spherical cells. The parameter α can be determined from the flux matching condition, $D\alpha r_0^{-2} = \Psi$, and we have

$$\overline{u} = \frac{\Psi r_0}{D} + \frac{K_m}{\rho_{\mathrm{TR}} \widehat{\psi} / \Psi - 1} , \tag{3.10}$$

where the flux is diffusion-limited if the first term on the right dominates, and the flux is machinery-limited if the second term dominates.

In the diffusion-limited regime $\Psi \approx D\overline{u}/r_0$ and $u(r_0) \ll \overline{u}$, whereas in the machinery-limited regime, $\Psi \ll D\overline{u}/r_0$ and $u(r_0) \approx \overline{u}$. In the latter, Ψ increases in proportion to ρ_{TR} and the flux Ψ is separable into a factor ρ_{TR} that depends on building block investment, which is controlled by the cell itself, and a factor $\widehat{\psi}/(1 + K_m/\overline{u})$ that depends on the environment. However, every increase of ρ_{TR} moves the system closer to its transition to the diffusion-limited regime and accordingly the flux gains per building block invested steadily diminish.

From a mechanistic point of view, the single-envelope uptake system is much less intricate than the dual-envelope systems. Notwithstanding these differences, the phenomenological equations obtained on the balancing principle are identical. If we posit a linear budgeting constraint, together with $\mu \propto \Psi_{\mathrm{A}}$, $\mu \propto \Psi_{\mathrm{B}}$, we recover an expression formally identical to equation (3.5) (although the compound parameters now have a different interpretation in terms of the underlying mechanistic-biochemical parameters). Similarly, the minimum model, equation (3.7) is obtained via the same argument as presented in Section 3.2, and the general equations (3.6) and (3.8) ensue as well.

In summary, both for the Gram-negative dual-envelope system (Type I Holling response) and the Gram-positive single-envelope system (Type II Holling response) we derive, at the whole-organism level of biomass increase, hyperbolic ('Monod') responses when diffusion is non-limiting and responses of the 'minimal model' kind when diffusion is the dominating factor.

3.4 *Adaptation of the Type I response relationship*

Let us consider a system in which the relationship between the flux Ψ and the limiting nutrient concentration $\overline{u}$ is the Holling Type I response as depicted in Fig. 2. By the argument given in Section 3.1, the optimal investment of molecular building blocks into machinery should be such that the transition point in the Type I response (where the initial slanted portion connects to the constant portion) occurs just at the prevailing value of $\overline{u}$.

Furthermore, if dynamic re-allocation of building blocks takes place, the Type I response curve should itself shift as the organism, previously acclimatised to ambient concentration $\overline{u}_1$ is now exposed to a different concentration $\overline{u}_2$ and allowed to adapt to this new environment. For instance, if $\overline{u}_2 < \overline{u}_1$, we should expect a greater investment of building blocks to porins, and hence less machinery can be devoted to growth.

Thus far we have been concerned with 'top-down' arguments in the spirit of optimal foraging ideas. We are yet to supply 'bottom-up' arguments that explain how the cell might in fact accomplish such optimal re-allocation of building blocks. In other words, we should establish that dynamic re-allocation is mechanistically plausible. To this end, we previously proposed a theory geared to provide such a

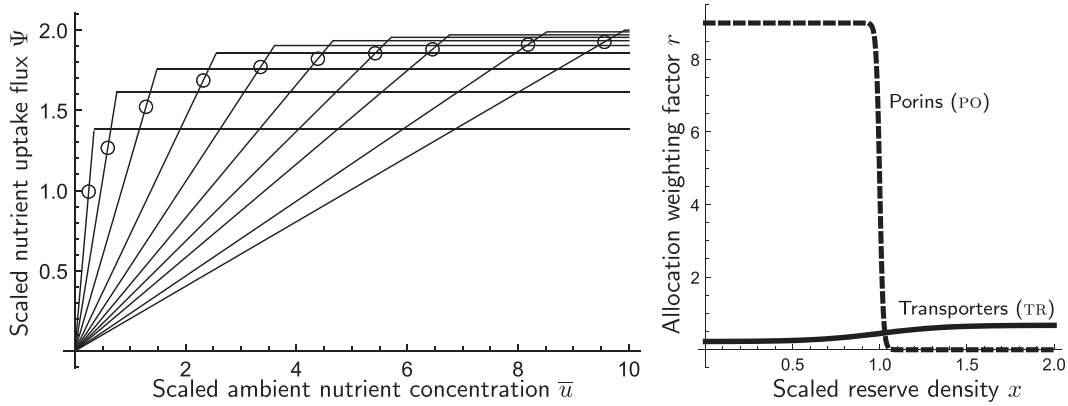

FIG. 4. Steady-state response of simulation model, showing the Type-I response at various nutrient concentrations. Further explanation in the text; governing equations of the simulation model are detailed in Appendix A.

mechanistic underpinning (Nev & van den Berg, 2017a,b), in which we express allocation of building blocks towards machinery of type i in terms of a dimensionless constant $\alpha_i \in [0, 1]$, where the α_i sum to 1 over all types of machinery. We proposed a 'ribosome time-sharing formula' $\alpha_i = r_i/r_T$, where $r_i \geqslant 0$ and r_T is a normalisation factor, specifically the sum of the r_i over all types of machinery. The quantity r_i is assumed to depend on factors that can be sensed by the machinery that controls the transcription of genes. For example, if the machinery at hand is the uptake machinery for the nutrient, we take r_i to be a sigmoid decreasing function of the reserve density. As the latter goes down, r_i will go up and so will α_i: more is invested into uptake and the reserve density will tend to go up. This arrangement essentially constitutes a negative feedback loop.

To assess whether this simple feedback loop can regulate the porin/transporter system, several simulations were run, the results of which are shown in Fig. 4 (see Appendix A for further details of the simulations). Each of the Type I responses shown is the relationship after the simulated organism has been allowed to adapt to the prevailing value of $\overline{u}$; the realised flux at that value is indicated by a circle, which labels each graph with the $\overline{u}$ for which it was obtained. As $\overline{u}$ decreases, allocation to porins increases and to transporters decreases; thus the initial slanted portion becomes steeper and the constant portion gradually lowers. This is the basic trade-off that was described in Section 3.1.

It can be seen that the model is not quite perfect, since by the foregoing arguments the circles indicating the flux at the prevailing nutrient concentration ought to be located exactly at the transition point (the 'kink'). The r_i-functions for this model are shown in the panel on the right: the porins are governed by the classical negative feedback relationship, whereas the transporters are governed by an *increasing* sigmoid function.

4. Diffusion relationships

In the foregoing we used several expressions describing physical relationships related to diffusion of the nutrient in the medium surrounding the bacterial cell; in the present section we outline a more detailed justification for these expressions.

4.1 *Diffusion of nutrient in the extracellular medium*

We assume that passive transport from the bulk of the medium towards the outer surface of the cell proceeds down a concentration profile that satisfies the Laplace equation $\Delta u = 0$. For a spherical cell whose outer surface is uniformly covered with uptake machinery, it is reasonable to assume that the geometry is radially symmetric. In spherical coordinates, the Laplace equation reads

$$u''(r) + 2r^{-1}u'(r) = 0\,, \tag{4.1}$$

where u is a function of radial distance r alone. This ordinary differential equation is satisfied by $u(r) = \overline{u} - \alpha/r$ where α is a constant that is yet to be determined. Here, $\lim_{r\to\infty} u(r) = \overline{u}$, which we interpret as the bulk concentration of the ambient medium. For $\alpha > 0$ the concentration $u(r)$ decreases as one moves towards the cell, which is what we require for net transport to be in that direction.

Growing bacterial cells divide and form colonies, and these may themselves form spherical masses; this poses a special difficulty since only the cells on the outer surface face conditions as described by the above equation. These bacterial colonies may also form filamentous structures, which can be conceptualised as cylinders and thus described by the Laplace equation in cylindrical coordinates:

$$u_{rr}(r,z) + r^{-1}u_r(r,z) + u_{zz}(r,z) = 0\,, \tag{4.2}$$

where r is the radial coordinate and z is the coordinate pointing along the axis of the filament; subscripts here denote partial derivatives. The term u_{zz} becomes important near the ends of the filament but can be treated as negligible for a 'typical' cell somewhere along the filaments, away from its ends. The dependence on z can therefore be ignored, leaving a radial equation:

$$u''(r) + r^{-1}u'(r) = 0\,, \tag{4.3}$$

which is satisfied by the expression $u(r) = \overline{u} - \alpha \ln\{\overline{r}/r\}$, where $\overline{r}$ denotes the distance between the centreline of the filament and the boundary between the unstirred layer near the cells and the well-stirred bulk phase of the medium. At $r = \overline{r}$, we have $u = \overline{u}$, which is the value the bulk has throughout. The flux matching condition becomes $\Psi = D\alpha/r_0$ and hence $u(r_0) = \overline{u} - \alpha \ln\left\{\overline{r}/r_0\right\} = \overline{u} - \Psi r_0 D^{-1} \ln\left\{\overline{r}/r_0\right\}$. It follows that the same relationships ensue if D/r_0 is replaced throughout by $\widetilde{D}/r_0$ where $\widetilde{D} = D/\ln\left\{\overline{r}/r_0\right\}$; the sole difference between the spherical and the cylindrical geometry amounts to a rescaling of the diffusion constant.

4.2 *The escape probability*

To motivate (2.4) we develop a partially heuristic argument based on potential theory. Let $P_{\rm esc}(\boldsymbol{r})$ denote the probability that a nutrient particle, not (yet) ligated to a binding protein, and located at position $\boldsymbol{r}$ within the PS, will leave the PS via one of the pores in the OM, rather than be captured by a binding protein and subsequently delivered to a transporter. Let $S_{\rm PO}$ and $S_{\rm BP}$ be subsets of $\mathbb{R}^3$, defined as follows:

$$S_{\rm PO} = \{\boldsymbol{r} : |\boldsymbol{r}_{\rm PO} - \boldsymbol{r}| \leqslant R_{\rm PO}\}\,, \qquad S_{\rm BP} = \{|\boldsymbol{r}_{\rm BP} - \boldsymbol{r}| \leqslant R_{\rm BP}\}\,, \tag{4.4}$$

where $\boldsymbol{r}_{\rm PO}$ is the centre of a pore with interaction radius $R_{\rm PO}$, and $\boldsymbol{r}_{\rm BP}$ is the centre of a binding protein with interaction radius $R_{\rm BP}$. Provided that the subsets $S_{\rm PO}$ and $S_{\rm BP}$ are disjoint, an elegant argument based

on conditioning (see, for instance, Grimmett & Stirzaker, 1992 512ff.) establishes that $P_{\rm esc}(\boldsymbol{r})$ satisfies the Laplace equation $\Delta P_{\rm esc}(\boldsymbol{r}) = 0$ at all points $\boldsymbol{r} \notin S_{\rm PO} \cup S_{\rm BP}$, with the boundary conditions

$$P_{\rm esc}(\boldsymbol{r}) = \begin{cases} 0 & \text{if } \boldsymbol{r} \in S_{\rm BP} \\ 1 & \text{if } \boldsymbol{r} \in S_{\rm PO} \end{cases}.$$

The situation is rather more complicated as pores and binding proteins are both present in multiple copies, and the binding proteins are themselves presumably performing a random walk in the PS. A direct approach would be to extend the definitions (4.4) to include all these molecules, and effectively treat $S_{\rm BP}(t)$ as a time-dependent stochastic process variable. We avoid this direct approach by thinking of the escape probability relative to a porin as an electric field and attempting to estimate the 'typical' screening off of this field due to the porins in the mean field.

Accordingly, let us focus on a single pore, which we think of as the nearest one to the particle of interest (and therefore exerting a dominant influence on its escape probability) and let r denote the distance to this pore. The pore can be represented by a point charge $q_{\rm eff}$, placed at its centre and chosen such that $P_{\rm esc} = 1$ at a distance $R_{\rm PO}$ from the pore's centre. A binding protein at distance r from the pore is represented by a sphere with radius $R_{\rm BP}$, on the surface of which the escape probability equals zero. Thus, if the particle approaches a binding protein to within distance $R_{\rm BP}$ of the latter's centre of mass, we posit that it is certain to be bound—that is, $R_{\rm BP}$ represents the *capture radius* of the binding protein, with $P_{\rm esc} = 0$ on the surface of the sphere. Similarly, $R_{\rm PO}$ represents the capture radius of the pore. Now it turns out that the sphere can be replaced by a point charge q' placed inside the sphere, in the sense that the potential associated with the two point charges $q_{\rm eff}$ and q' also vanishes on the surface of the sphere, thus satisfying the same boundary conditions (see, for instance, Griffiths, 1999, 124ff.). Specifically, the 'image' charge is given by $q' = -q_{\rm eff} R_{\rm BP}/r$ and it is located at a distance $R_{\rm BP}^2/r$ from the centre of the sphere along the axis that connects the centres of the porin and the binding protein (Fig. 5).

The next step is to introduce a mean field *as well as* a far field simplification. The mean field simplification is to work with the expected amount of screening off due to binding proteins. In a spherical shell of thickness dr at a distance r from the pore, there are on average $\rho_{\rm BP}^{\rm free} 4\pi r^2 dr$ binding proteins, all contributing to a mean field screening effect. As we move away from the pore, the contribution due to binding proteins on the shell at the closer distance r will assume a far field character, that is,

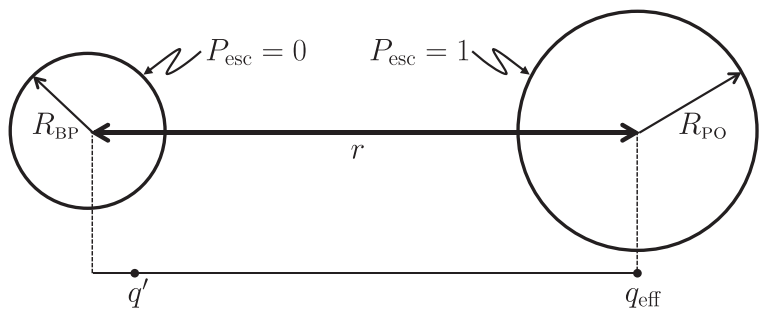

FIG. 5. A binding protein located at distance r from a porin. The capture radii $R_{\rm BP}$ and $R_{\rm PO}$ define spherical surfaces on which the escape probability $P_{\rm esc}$ equals 0 and 1, respectively, setting up a problem in which $P_{\rm esc}$ at any position outside these spheres can be described by a corresponding potential. The problem is equivalent to a simpler problem with point charges $q_{\rm eff}$ and q'. Representative values are $R_{\rm PO} \gtrsim 5$ nm and $R_{\rm BP} \gtrsim 2$ nm; see Appendix B for more details.

their collective charge can simply be added to the effective charge q_{eff}. Putting these ideas together and writing P_{esc} for the effective charge q_{eff} plus the 'screening off' contributions from binding proteins closer to the porin, we arrive at the following ordinary differential equation:

$$\frac{\mathrm{d}P_{\text{esc}}(r)}{\mathrm{d}r} = -P_{\text{esc}}(r)\frac{R_{\text{BP}}}{r}4\pi r^2\rho_{\text{BP}}^{\text{free}} = -4\pi P_{\text{esc}}(r)R_{\text{BP}}\rho_{\text{BP}}^{\text{free}} r\,, \tag{4.5}$$

with initial condition $P_{\text{esc}}(R_{\text{PO}}) = 1$. The solution for $r \geqslant R_{\text{PO}}$ can be written as follows:

$$\ln P_{\text{esc}}(r) = -2\pi R_{\text{BP}}\rho_{\text{BP}}^{\text{free}}\left(r^2 - R_{\text{PO}}^2\right)\,. \tag{4.6}$$

This describes the escape probability for a nutrient particle at distance r from the nearest pore. To find the escape probability for a nutrient particle chosen at random, we must average the above formula over the distribution for the distance of such a particle to the nearest porin. A particle that has just entered the PS will still be fairly close to the OM, so we assume that the distance to the OM is negligible, which allows us to treat the problem as two-dimensional. Thus, we consider the probability $S(r)$ that the nearest pore is located *further away* than r as measured from an arbitrary test location on the OM. This probability satisfies the differential equation

$$S'(r) = -2\pi r\rho_{\text{PO}}S(r)\,, \tag{4.7}$$

since the expected number of pores encountered in an annulus of width $\mathrm{d}r$ at distance r equals $\rho_{\text{PO}}2\pi r\mathrm{d}r$. The solution of equation (4.7) with initial condition $S(0) = 1$ is $\ln S(r) = -\pi\rho_{\text{PO}}r^2$. Finally, the expected 'pore charge' a free nutrient particle senses is estimated by taking the expectation of $P_{\text{esc}}(r)$, equation (4.6), using the statistics of the pore distance:

$$P_{\text{esc}} = \int_{R_{\text{PO}}}^{\infty} S'(r)\exp\left\{-2\pi R_{\text{BP}}\rho_{\text{BP}}^{\text{free}}\left(r^2 - R_{\text{PO}}^2\right)\right\}\mathrm{d}r = \frac{\exp\left\{-\pi\rho_{\text{PO}}R_{\text{PO}}^2\right\}}{1 + 2R_{\text{BP}}\rho_{\text{BP}}^{\text{free}}/\rho_{\text{PO}}}\,. \tag{4.8}$$

Setting the exponential factor to 1, since R_{PO} is small, we obtain equation (2.4) with $\delta = 2R_{\text{BP}}$; however, we should not expect this last equality to be exact, in view of the various drastic simplifications we have made along the way. To verify the form of equation (2.4), the escape probability was estimated more directly by means of Monte-Carlo simulations. Results are shown in Fig. 6; the qualitative agreement with the heuristic formula is good, although the 'empirical' value of δ is quite different. Appendix B discusses representative dimensions of the relative sizes of porins, binding proteins and the PS. Using these data and taking the width of the PS as the natural unit of length, plausible estimates are $R_{\text{PO}} \gtrsim 0.25$ and $R_{\text{BP}} \gtrsim 0.1$.

5. Concluding remarks

The analysis presented in this paper would suggest that the Holling Type I functional response for nutrient uptake should not be uncommon in Gram-negative bacteria, and yet this response seems to have received little attention in the microbiological literature, despite its status as a standard concept in general ecology (Begon *et al.*, 1990). One obvious reason is that the classic Type I response requires ρ_{BP} to be substantial; otherwise the difference with the standard hyperbola will not readily be discerned

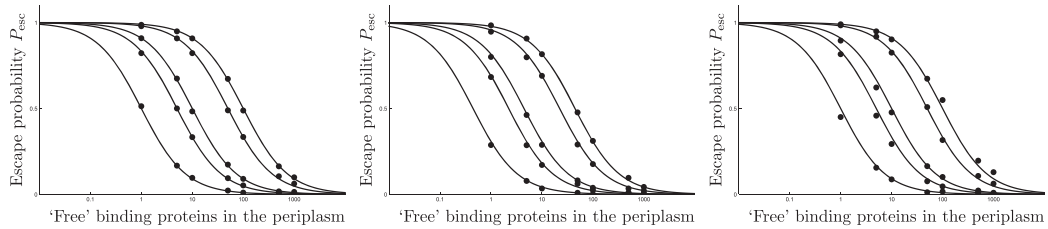

FIG. 6. Monte-Carlo estimations of the escape probability P_{esc} (dots), together with the approximate analytical expression, equation (2.4) (solid lines) for various densities of porins and binding proteins. The width of the periplasm has been assumed to equal 21 nm. Left: densities of porins corresponding to each curve are as follows (from left to right): $23/\mu m^2$, $115/\mu m^2$, $230/\mu m^2$, $1150/\mu m^2$, $2300/\mu m^2$; $R_{PO} = 1.05$ nm; $R_{BP} = 0.525$ nm; $\delta = 21$ nm. Middle: densities of porins corresponding to each curve are as follows (from left to right): $23/\mu m^2$, $115/\mu m^2$, $230/\mu m^2$, $1150/\mu m^2$, $2300/\mu m^2$; $R_{PO} = 1.05$ nm; $R_{BP} = 1.05$ nm; $\delta = 47.25$ nm. Right: densities of porins corresponding to each curve are as follows (from left to right): $2.5/\mu m^2$, $12.5/\mu m^2$, $25/\mu m^2$, $125/\mu m^2$, $250/\mu m^2$ (from left to right); $R_{PO} = 5.25$ nm; $R_{BP} = 2.1$ nm; $\delta = 21$ nm.

on this basis of experimental data subject to measurement noise (a secondary consideration is that transformations to linearity are often used, and these lead to systematic errors in parameter estimation). There appears to be a paucity of systematic studies in which porins, binding proteins and transporters are over- or under-expressed, separately or in combination. We suggest that such studies will reveal more complex relationships, in line with the theory proposed here, between these three parameters and the realised flux.

Acknowledgements

Comments and suggestions from two anonymous reviewers helped improve the presentation of this paper considerably.

Funding

EU Research Framework programme 7 *Marie Curie Actions* (316630 to O.A.N.), Centre for Analytical Science Innovative Doctoral Programme (CAS-IDP).

REFERENCES

BEGON, M., HARPER, J. L. & TOWNSEND, C. R. (1990) *Ecology: Individuals, Populations and Communities*. New York: John Wiley & Sons.

BERG, H. C. & PURCELL, E. M. (1977) Physics of chemoreception. *Biophysical J.*, **20**, 193–219.

BUTTON, D. K. (1998) Nutrient uptake by microorganisms according to kinetic parameters from theory as related to cytoarchitecture. *Microbiol. Mol. Biol. Rev.*, **62**, 636–645.

DAVIDSON, A. L. & CHEN, J. (2004) ATP-binding cassette transporters in bacteria. *Ann. Rev. Biochem.*, **73**, 241–268.

DROOP, M. R. (1968) Vitamin B12 and marine ecology. IV. The kinetics of uptake, growth and inhibition in *Monochrysis lutheri*. *J. Mar. Biol. Assoc.*, **48**, 689–733.

DWYER, M. A. & HELLINGA, H. W. (2004) Periplasmic binding proteins: a versatile superfamily for protein engineering. *Curr. Opin. Struct. Biol.*, **14**, 495–504.

ERICKSON, H. P. (2009) Size and shape of protein molecules at the nanometer level determined by sedimentation, gel filtration, and electron microscopy. *Biol. Proced. Online*, **11**, 32–51.

GOTTSCHAL, J. C. (1992) Continuous culture. *Encyclopedia of Microbiology*, vol. 1 (J. Lederberg ed.). San Diego, CA: Academic Press, pp. 559–572.

Graham, L. L., Beveridge, T. J. & Nanninga, N. (1991a) Periplasmic space and the concept of the periplasm. *Trends Biochem. Sci.*, **16**, 328–329.

Graham, L. L., Harris, R., Villiger, W. & Beveridge, T. J. (1991b) Freeze-substitution of Gram-negative Eubacteria: general cell morphology and envelope profiles. *J. Bacteriol.*, **173**, 1623–1633.

Griffiths, D. J. (1999) *Introduction to Electrodynamics*, 3rd edn. Upper Saddle River, New Jersey: Prentice-Hall International, Inc.

Grimmett, G. R. & Stirzaker, D. R. (1992) *Probability and Random Processes*, 2nd edn. Oxford: Oxford University Press.

Grover, J. P. (1991) Resource competition in a variable environment: phytoplankton growing according to the Variable-Internal-Stores model. *Amer. Nat.*, **138**, 811–835.

Jap, B. K. & Walian, P. J. (1990) Biophysics of the structure and function of porins. *Quart. Rev. Biophys.*, **23**, 367–403.

Jordy, M., Andersen, C., Schülein, K., Ferenci, T. & Benz, R. (1996) Rate constants of sugar transport through two LamB mutants of *Escherichia coli*: comparison of wild-type maltoporin and LamB of *Salmonella typhimurium*. *J. Mol. Biol.*, **259**, 666–678.

Koebnik, R., Locher, K. P. & Van Gelder, P. (2000) Structure and function of bacterial outer membrane proteins: barrels in a nutshell. *Mol. Microbiol.*, **37**, 239–253.

Kooijman, S. A. L. M. (2009) *Dynamic Energy Budget Theory for Metabolic Organisation*. New York: Cambridge University Press.

Kramer, G., Sprenger, R. R., Nessen, M. A., Roseboom, W., Speijer, D., de Jong, L., de Mattos, M. J. T., Back, J. & de Koster, C. G. (2010) Proteome-wide alterations in *Escherichia coli* translation rates upon anaerobiosis. *Mol. Cell. Proteomics*, **9**, 2508–2516.

Li, G.-W., Burkhardt, D., Gross, C. & Weissman, J. S. (2014) Quantifying absolute protein synthesis rates reveals principles underlying allocation of cellular resources. *Cell*, **157**, 624–635.

Liebermeister, W., Noor, E., Flamholz, A., Davidi, D., Bernhardt, J. & Milo, R. (2014) Visual account of protein investment in cellular functions. *Proc. Natl. Acad. Sci. U.S.A.*, **111**, 8488–8493.

Marr, A. G., Nilson, E. H. & Clark, D. J. (1962) The maintenance requirement of *Escherichia coli*. *Ann. N. Y. Acad. Sci*, **102**, 536–548.

Matias, V. R. F., Al-Amoudi, A., Dubochet, J. & Beveridge, T. J. (2003) Cryo-transmission electron microscopy of frozen-hydrated sections of *Escherichia coli* and *Pseudomonas aeruginosa*. *J. Bacteriol.*, **185**, 6112–6118.

Michaelis, L. & Menten, M. L. (1913) Die Kinetik der Invertinwirkung. *Biochem. Z.*, **49**, 333–369.

Monod, J. (1949) The growth of bacterial cultures. *Annu. Rev. Microbiol.*, **3**, 371–394.

Nev, O. A., Nev, O. A. & van den Berg, H. A. (2017) Optimal management of nutrient reserves in microorganisms under time-varying environmental conditions. *J. Theor. Biol.*, **429**, 124–141.

Nev, O. A. & van den Berg, H. A. (2017a) Microbial metabolism and growth under conditions of starvation modelled as the sliding mode of a differential inclusion. *Dyn. Systems*, doi:10.1080/14689367.2017.1298726.

Nev, O. A. & van den Berg, H. A. (2017b) Variable-Internal-Stores models of microbial growth and metabolism with dynamic allocation of cellular resources. *J. Math. Biol.*, **74**, 409–445.

Nikaido, H. (2003) Molecular basis of bacterial outer membrane permeability revisited. *Microbiol. Mol. Biol. Rev.*, **67**, 593–656.

Pirt, S. J. (1965) The maintenance energy of bacteria in growing cultures. *Proc. Roy. Soc. Lond.*, **133**, 300–302.

Schlegel, H. G. & Zaborosch, C. (1993) *General Microbiology*, 7th edn. Cambridge: Cambridge University Press.

Stock, J. B., Rauch, B. & Roseman, S. (1977) Periplasmic space in *Salmonella typhimurium* and *Escherichia coli*. *J. Biol. Chem.*, **252**, 7850–7861.

Tam, R. & Saier Jr., M. H. (1993) Structural, functional, and evolutionary relationships among extracellular solute-binding receptors of bacteria. *Microbiol. Rev.*, **57**, 320–346.

van den Berg, H. A. (2011) *Mathematical Models of Biological Systems*. New York: Oxford University Press.

van Wielink, J. E. & Duine, J. A. (1990) How big is the periplasmic space? *Trends Biochem. Sci.*, **15**, 136–137.

Appendix A

The simulation model has been derived in detail in previous papers (Nev & van den Berg, 2017a,b; Nev *et al.*, 2017). The scaled (dimensionless) equations are as follows:

$$\dot{m}_0 = \alpha_0 m_0 - \psi_W m_G m_0 \tag{A.1}$$

$$\dot{m}_G = \alpha_G m_0 - \psi_W m_G^2 \tag{A.2}$$

$$\dot{m}_{\mathrm{PO}} = \alpha_{\mathrm{PO}} m_0 - \psi_W m_G m_{\mathrm{PO}} \tag{A.3}$$

$$\dot{m}_{\mathrm{TR}} = \alpha_{\mathrm{TR}} m_0 - \psi_W m_G m_{\mathrm{TR}} \tag{A.4}$$

$$\dot{x} = \min\left\{\bar{u} m_{\mathrm{PO}}, \psi_{\mathrm{TR}} m_{\mathrm{TR}}\right\} - \sigma m_0 - \psi_W m_G\,(1+x) \tag{A.5}$$

where the dot denotes differentiation with respect to time. The state variables are all densities (intensive variables) and are interpreted as follows: m_0: machinery-synthesising machinery; m_G: growth machinery; m_{PO}: porins; m_{TR}: transporters; x reserves. Not required but optional is an extensive state variable W corresponding to the structural biomass, which satisfies $\dot{W} = W\mu = W\psi_W m_G$; the saturating excess of binding protein is assumed to be an integral part of this structural component. The term $\min\left\{\bar{u} m_{\mathrm{PO}}, \psi_{\mathrm{TR}} m_{\mathrm{TR}}\right\}$ in equation (A.5) represents the Holling Type I functional response.

The allocation fractions are given by the formula $\alpha_\star = r_\star / r_T$ where $\star \in \{0, G, \mathrm{PO}, \mathrm{TR}\}$ with

$$r_0 = 1\,, r_G = (1+\exp\{(1-m_0)/\varepsilon_0\})^{-1}\,, r_{\mathrm{PO}} = \widehat{r}_{\mathrm{PO}}(1+\exp\{(x-1)/\varepsilon_{\mathrm{PO}}\})^{-1}\,,$$
$$r_{\mathrm{TR}} = \check{r}_{\mathrm{TR}} + \widehat{r}_{\mathrm{TR}}(1+\exp\{(1-x)/\varepsilon_{\mathrm{TR}}\})^{-1}\,. \tag{A.6}$$

The following parameter values were used for the results shown in Fig. 4: $\psi_W = 1$; $\psi_{\mathrm{TR}} = 4.325$; $\sigma = 1$; $\varepsilon_0 = 0.2$; $\varepsilon_{\mathrm{PO}} = 0.01$; $\varepsilon_{\mathrm{TR}} = 0.19$; $\widehat{r}_{\mathrm{PO}} = 9$; $\widehat{r}_{\mathrm{TR}} = 0.45$; $\check{r}_{\mathrm{TR}} = 0.225$.

Appendix B

Periplasmic space A classic study estimates the PS to comprise from 20% to 40% of the total cell volume (Stock *et al.*, 1977). This range was deemed to be implausible given that it would imply a periplasmic thickness upwards from 32 nm in a typical Gram-negative bacterium (van Wielink & Duine, 1990), at odds with the evidence from electron microscopic studies, which would suggest ∼12 nm in conventionally fixed *Escherichia coli* cells (Graham *et al.*, 1991a); however, fixation by freeze substitution led to somewhat higher estimates, ranging between 10 nm and 26 nm, depending on the species concerned (Graham *et al.*, 1991b). More recent methods of fixation yielded a typical value of 21 nm for *E. coli*; it was observed that the thickness of the periplasm may vary even for an individual cell as the protoplast may be able to float freely within the periplasm (Matias *et al.*, 2003).

Porins Porins are barrel-shaped transmembrane proteins, standing ∼5 nm tall with a comparable width (Koebnik *et al.*, 2000; Nikaido, 2003), the bore diameter of the central channel measuring ∼1 nm (Jap & Walian, 1990; Nikaido, 2003). However, porins occur in trimeric complexes with a width of ∼ 10 nm (Jap & Walian, 1990) and the capture radius R_{PO} is determined by how closely a particle must venture near such a complex to virtually ensure capture and transport. Thus we should expect R_{PO} upwards from 5 nm, with a true (effective) value depending on the reach of the intermolecular forces between the porin complex and the nutrient particle.

BINDING PROTEINS Periplasmic solute binding proteins span a molecular weight range of 22 kDa to 45 kDa (Tam & Saier, 1993; Dwyer & Hellinga, 2004). Assuming these proteins to be globular and using the empirical formula given by Erickson (2009), one finds that this corresponds to a range of diameters between 3.7 nm and 4.8 nm. Thus we should expect R_{BP} upwards from 2 nm, with a true value depending on the reach of the intermolecular forces between the binding protein and the nutrient particle.